2021 43rd Annual International Conference of the
IEEE Engineering in Medicine & Biology Society (EMBC)
Oct 31 - Nov 4, 2021. Virtual Conference

A Novel Approach to Decode Covert Spatial Attention Using SSVEP and Single-Frequency Phase-Coded Stimuli

Alexandre Armengol-Urpi[1*], Andres F. Salazar-Gomez[2] and Sanjay E. Sarma[1]

***Abstract*— This paper investigates for the first time the use of single-frequency phase-coded stimuli to detect covert visuo-spatial attention (CVSA) with steady-state visual evoked potentials (SSVEP). Two 15Hz pattern-onset stimulations were encoded with opposite phases and simultaneously presented on a LCD monitor. The effects of attending each stimulus on the amplitudes and phases of the evoked SSVEPs across the visual cortex are explored. A real-time CVSA classification experiment was simulated offline with 9 BCI-naive subjects, achieving an average classification accuracy of 88.4 $\pm$ 8% SE. Our results are, to our knowledge, the first report that CVSA can be decoded with SSVEP using single-frequency phase-coded stimuli. This opens opportunities for attention-tracking applications with largely increased number of targets.**

I. Introduction

Covert Visuo-Spatial Attention (CVSA) is the human ability to commit attention to locations in the peripheral field of view without any overt eye movement [1]. CVSA is essential for many everyday activities, because it allows us to improve discriminability in visual tasks, such as contrast sensitivity [2], [3], texture segmentation [4], and visual search [5]. CVSA processes have been widely studied to understand how humans behave when performing certain cognitive visual tasks or activities [6]–[8]. Since covert shifts of attention cannot be observed externally, electroencephalography (EEG) provides access to these events [8]. One of the most used approaches to monitoring what locations in the visual field covertly receive spatial attention consists of studying how certain brainwaves respond to visual stimuli. It has been shown that neuronal responses to visual stimuli are amplified when attention is directed to the stimuli, compared to when the stimulus is unattended [9], [10]. In particular, Steady-State Visually Evoked Potentials (SSVEP) are one of the most widely used processes for this purpose due to their straightforward implementation and high signal-to-noise ratio (SNR).

SSVEP are oscillatory signals generated at the visual cortex that occur in response to visual stimulation at specific frequencies [11], [12]. When a person overtly or covertly shifts the attention to a particular flickering stimuli, the amplitudes of the evoked SSVEP increase with respect to when the stimuli is ignored [9], [13]. This has interested researchers in the field of Brain-Computer Interfaces (BCI). Since monitoring CVSA enables the creation of gaze-independent BCIs, it can allow severely disabled patients who cannot move their eyes to communicate, among other applications. In [14] and [15], the authors employed SSVEP modulations evoked by frequency-coded stimuli in the right and left periphery to detect which stimulus was covertly receiving the attention of the user. They used 10.03Hz and 12.04Hz as the stimulation frequencies. The authors in [9] studied the effects of selective attention on the SSVEP in the low-frequency range (8-12Hz), and the authors in [13] did a similar study in the mid-frequency range (20-28Hz). They all concluded that the SSVEP were modulated by CVSA.

Visual selective attention can be committed not only to spatial regions in the visual field but also to non-spatial features, like colors, motions, or orientations. This receives the name of Feature-Based Attention (FBA) and it functions independently of spatial attention [16]–[18]. Similarly to CVSA, FBA also increases neuronal responses in the brain regions that process the attended feature [19], [20]. This opens the door to other modalities of SSVEP-based BCIs, where the SSVEP modulations are evoked by shifts between visual features instead of spatial locations [7], [20], [21].

In order to increase the applicability of these systems, minimizing eye fatigue and user discomfort created by the flickering stimuli is a key factor. Thus, there is a recent trend among visually evoked potentials-based BCI researchers to utilize frequencies above the flicker fusion rate to make the stimuli imperceptible [22]–[25]. This requirement reduces considerably the number of possible different stimuli targets since the monitor refresh rate further limits the frequencies that can be rendered. In an effort to increase the number of targets for a single flickering frequency, our work explores incorporating *phase information* into the stimuli and decoding it from CVSA-enabled systems.

It is well known that SSVEPs are time and phase-locked to the stimuli [26], [27]. This characteristic has been widely exploited to develop SSVEP-based BCI systems with phase-coded stimuli [28]–[30]. However, to the best of our knowledge, phase has never been used as the target-encoding element in CVSA-enabled systems. This paper explores for the first time the use of covert visuo-spatial attention to discriminate single-frequency phase-coded stimuli using SSVEP and presents encouraging results for its implementation in BCIs.

*Corresponding author
[1]Department of Mechanical Engineering, Massachusetts Institute of Technology, Cambridge, MA 02139, USA
[2]MIT Open Learning, Massachusetts Institute of Technology, Cambridge, MA 02139, USA
Emails: armengol@mit.edu, salacho@mit.edu, sesarma@mit.edu

II. Methods

A. Participants

10 healthy subjects, age 25-36 (mean=29.3, SD=3.2) with normal or corrected-to-normal vision participated in this study. Subjects were seated in front of a monitor and placed their heads on a chin rest so that the distance and visual angles to the stimuli were kept constant. The chin rest was located 53 cm away from the monitor, as seen in Figure 1. The study was approved by the MIT Committee on the Use of Humans as Experimental Subjects.

B. Data Acquisition

EEG data was acquired using an Enobio system from Neuroelectrics [31] with 7 electrodes located in the parietal and occipital regions using the 10-20 distribution (PO3, PO4, PO7, PO8, O1, Oz, O2) at a sampling rate of 500Hz. The reference and ground electrodes were placed at FPz and left mastoid respectively. The electrooculogram (EOG) was recorded using two electrodes placed on either side of the eyes (i.e. outer canthi) to monitor lateral eye movements and blinks. To synchronize the EEG data with the stimulus onset, a photo-diode captured the changes in luminance of a dummy square that flickered with zero reference phase, and it was covered so that subjects could not see it.

C. Stimuli Design

The stimuli were presented by an LCD monitor with a refresh rate of 240Hz. As shown in Figure 2, the stimulus setup was formed by two flickering white squares, all flashing at 15Hz, and they were encoded by opposite phases (0 and π). The on-off duty cycles were 50/50 for both squares. Each square had a size of 200x200 pixels, which accounted for 6.7° of visual angles. A fixation cross was rendered at the center of the screen and the subjects were asked to maintain visual fixation on it. Black alphanumeric character sequences were superimposed on the flickering white squares, and had the function to capture the covert attention of the subjects. Inspired by the methodology in [9], the character sequence consisted of randomized displays of letters A to Z and the number 5, which was defined as the infrequent covert attention target, appearing with a probability of 0.08 per character. The sequence of characters was presented concurrently at the right and left positions, with a duration of 200 ms per character. Each visual field received a different randomized sequence per trial. The stimulation software was written in Matlab using the Psychophysics Toolbox [32].

D. Experimental Procedure

Each trial began with a countdown of 4 seconds, and either a left or right-pointing arrow indicated which sequence the subject had to commit attention to during that trial. Each stimulation trial was 7 seconds long. Subjects were asked to gaze at the central fixation cross during the 7 seconds and focus the attention on the corresponding character sequence. When a target character (”5”) was presented on the attended sequence, subjects had to press the space bar of a keyboard, and the response times were recorded. The responding hand

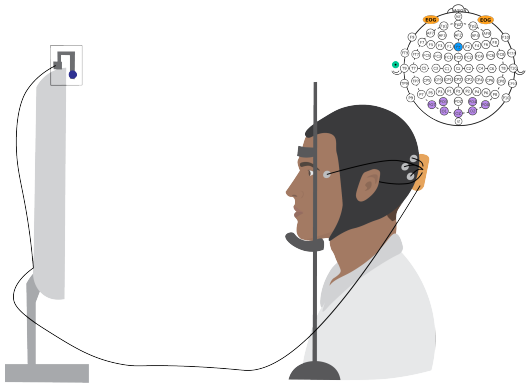

Fig. 1: Experimental setup. A photo-diode (upper left) was used to synchronize the stimulation trials with the captured data. Top right drawing shows the EEG electrodes placement according to the international 10-20 system. Colors represent data channels (purple), reference (blue), ground (green) and EOG (yellow) electrodes.

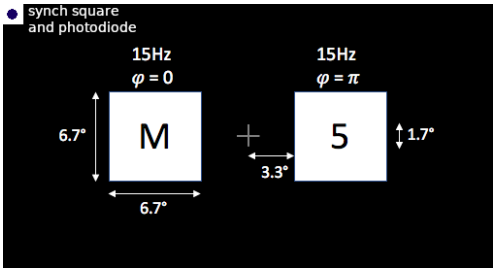

Fig. 2: Visual display utilized in the experimental sessions. A synchronization square was located at the top-left corner of the display, and it was covered so that subjects could not see it.

was counterbalanced across experimental trials. Subjects were asked to avoid blinks or head movements during the 7-second stimulation. Trials were recorded in blocks of 20 – 10 attending left square and 10 attending right square, sequentially alternating between left and right. Each block was repeated 10 times, so the whole experiment consisted of 200 7-second individual trials, 100 for each location.

At the end of the main 10 blocks, an extra 20-trial block with single-stimulus was recorded with 10 trials only showing the cued left targets (and no flickering square on the right), and 10 trials with only the cued right targets (no flickering square on the left) . This allowed us to capture the evoked SSVEPs without the effect of the unattended square.

The experiment started with an introductory session for baseline recording, alpha waves monitoring and EOG calibration. The total duration of an experiment was approximately 90 minutes.

E. Trial rejections

An important data selection process is to remove trials in which the user is not properly attending the cued square. To identify them, key-press response times following target (”5”) onset were measured. If the response time was not

within a 200ms-1200ms interval after onset, it was marked as a missed target. The averaged percentage of correct target detections across subjects was 76.2%, with a standard error of 4.43%. If, within a 7-second trial, more than half of the targets were missed, we categorized the subject as not paying enough attention during the sequence, and that trial was rejected. Across subjects, an average of 17.8 trials were rejected (8.9%).

Trials with undesired eye movements had to be rejected as well. The EOG signals were analyzed offline to consider 3 undesired events: eye blinks, eye saccades (or gaze jumps) and smooth pursuit eye movements. The calibration session was designed to characterize the EOG of undesired events that could affect the EEG data. The whole trial was rejected if any of these 3 EOG patterns was detected during the visual inspection. Across subjects, an average of 15.8 trials were rejected. One of the subjects presented difficulties to get a good ground electrode contact, which was reflected on the overall quality of the EEG and EOG data captured. Hence, we decided to remove this subject from the data set.

F. Time-domain Averaging Analysis

In this study all analysis was done offline. Epochs for each 7-second trial were extracted (from 0 - 7000 ms post-target onset time) and band-pass filtered using a 4th order Butterworth zero-phase filter with a passband of 5-60 Hz. Then, trials corresponding to ”attend left” and ”attend right” were averaged separately in the time domain. Hence, two 7-second averaged epochs were obtained per subject at each scalp site. To extract the resultant phases and amplitudes of the evoked SSVEP, a 3-second moving window with steps of 200ms was applied to the 7s averaged epochs. For each of the windowed 3-second epochs, amplitude and phase of the 15Hz SSVEP were computed at each scalp site using the Fast Fourier Transform (FFT). SSVEP amplitudes were calculated normalizing by the number of FFT samples to obtain results in microvolts, and phases were computed from the ratio of the signed real and imaginary components. For each subject, 22 amplitude-phase pairs were obtained. Polar plots of these epochs for a particular subject can be seen in Figure 3a, revealing that the distribution of the points is dependant on the attention side of the subject.

G. Real-time Analysis

We explored the feasibility of detecting the subject's covert attention in real-time. We simulated a real-time scenario during offline analysis.

A moving window of N seconds and steps of 200ms was applied to each one of the 7-second individual trials, where N varied from 0.5 to 5 seconds. Similarly as in the Time-domain Averaging Analysis (Section II-F), for each of the windowed N-second epochs, amplitude and phase of the 15Hz SSVEP were computed at each scalp site using the FFT. From the polar plots shown in Fig 3a, we can see that the 2D positions of the amplitude-phase points for each scalp site vary with the attention site. Thus, x-y coordinates of the amplitude-phase plot for each channel

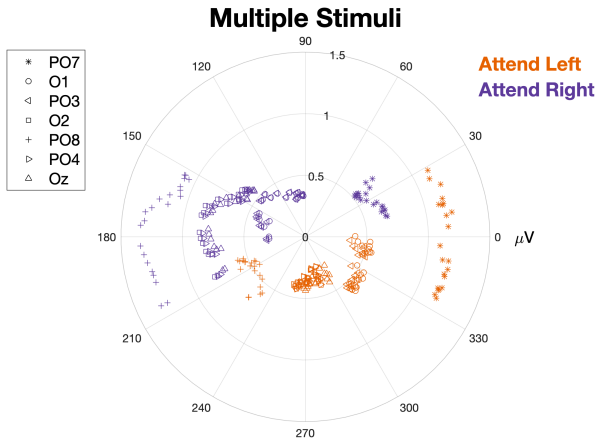

(a) Both stimuli simultaneously. Attention target cue was left (orange) or right (purple) square.

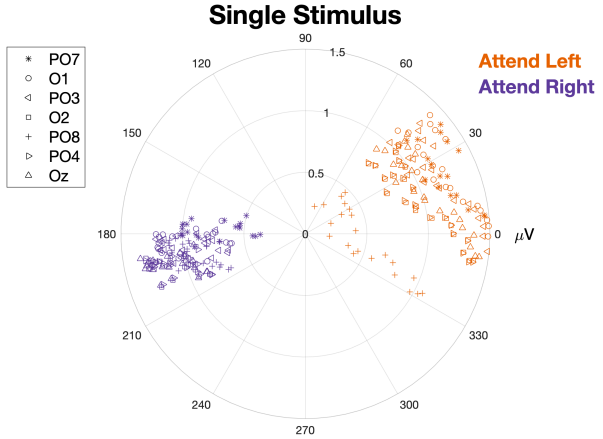

(b) Single-stimulus trials. Attention target cue was left (orange) or right (purple) square. Notice the 180-degree offset between point clouds for the left and right stimulus.

Fig. 3: SSVEP amplitudes (μV) and phases (deg) for all the 7 electrodes of windowed 3-second epochs obtained from time averaged trials for subject number 3, for multiple (3a) and single-stimuli (3b) conditions.

epoch were used as features for the classifier. To extract more information from each epoch, amplitude and phase of the first SSVEP harmonic (30Hz) were also computed and included as features. This way, one feature vector consisted of 28 features (2 features per scalp site and frequency). The number of data points varied depending on the moving window length, spanning from 1,200 to 3,500 for each class and subject. All features were normalized and standardized (z-scored).

A 10-fold cross validation paradigm was implemented for the train-test procedure. A logistic regression classifier was chosen since it showed good performance and is the most parsimonious classifier for binary classification.

III. Results

A. Time-domain Averaging

The SSVEP amplitudes and phases from each subject can be plotted on the imaginary plane using polar coordinates.

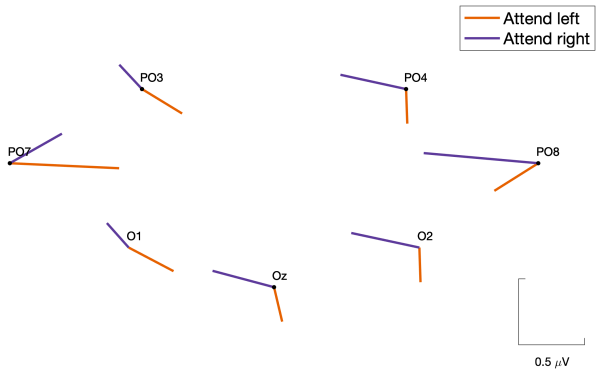

Fig. 4: Amplitudes and phases of resultant 15Hz SSVEPs from subject 3 plotted in polar coordinates on each scalp site. Amplitudes are represented by line length. Phases are plotted with cosine-onset convention with 0° to the right and +90° upwards. PO8 and PO7 show opposite behavior, suggesting the effect of visuo-spatial attention directionality on the signal's phase.

These polar plots show how these amplitude-phase pairs are distributed depending on which target the subject was covertly attending to. An example of such plots for one subject can be seen in Fig 3a. Each dot or vignette represents the polar coordinates (magnitude and phase) from an electrode's windowed 3-second epoch. Color represents the attended square. We can see how data-points are clustered for each scalp site, proving that the computed phases and amplitudes are consistent during the trial. Within a particular attending condition (attend left or right), it can be seen that the topography of the SSVEPs changes across the scalp. For example, the responses in the most lateral regions at opposite hemispheres oscillate with opposite phases (PO7 vs. PO8). This can be due to the role of the optic chiasm in the vision pathway [33]. It can also be seen that all scalp site point clouds drift to the same direction on the imaginary plane when subject attends to the left or right stimulus. This suggests that it is indeed possible to discriminate where in the visual field the user is covertly directing the attention by phase-coding the stimuli and analyzing the position of the amplitude-phase pairs in the polar plot. For comparison purposes, similar plots were obtained from the average of the 10 trials that had been recorded with only the cued square appearing on the display, i.e. with single stimulus (3b).

In order to quantify the change in amplitude and phase of the SSVEP waves between the cue-left and cue-right epochs, the centroid of each scalp site point-cloud was computed. In Figure 4, amplitudes and phases of the averaged SSVEPs for each scalp site are shown. PO7 and PO8 show opposite behavior, suggesting the effect of visuo-spatial attention directionality on the signal's phase. In Figure 5 we show the displacement vectors representing the drift of amplitude-phase data points in the polar plane when subjects switch attention from left to right stimulus. Left to right criterion was chosen arbitrarily. This switch in attention is subject-specific, i.e. each subject has their own orientation. As seen, there is a common "flow" across all scalp sites, so there is

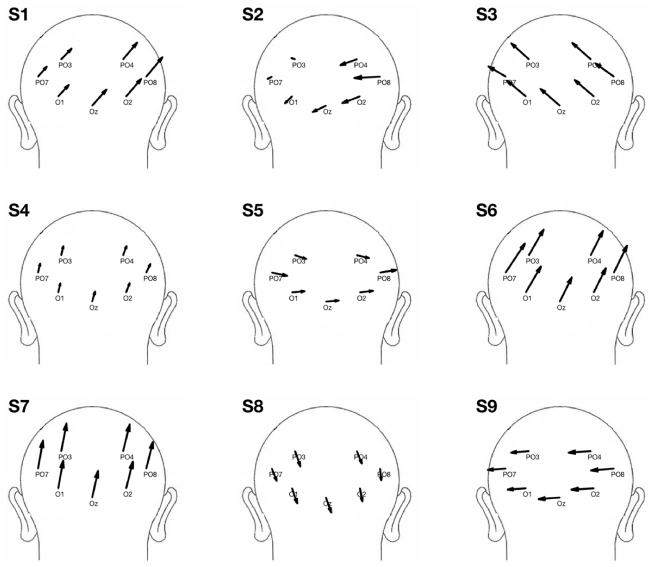

Fig. 5: Vectors representing the drift of amplitude-phase datapoints in the polar plane at each scalp site when subjects switch attention is from left to right stimulus. A common flow can be seen across all scalp sites within each subject. Flow orientation is subject-dependent.

similar amplitude-phase change at the measured visual cortex regions when the subject covertly changes the attention location. This suggests that the centroid of the 7 points could be used as a feature to discriminate what stimulus the subject is attending to.

The absolute change in amplitudes and phases was computed for each channel and subject in order to quantify how much each scalp region reacts to the change of attention side (left to right). Absolute values of the differences (attend left - attend right) were taken. An ANOVA test was performed to explore whether the amplitude and phase shifts of the averaged trials were more prominent in certain scalp sites. ANOVA tests ($N = 9, df = 6$) showed no significance for both amplitudes and phases shifts ($p > 0.05$ for both cases). Therefore, all cortical regions, across subjects, exhibit comparable changes in both SSVEP amplitudes and phases when attention side is switched. A bar chart with the averages across subjects can be visualized in Figure 6.

To visualize more general behavior of the SSVEP responses, we computed the centroids of the amplitude-phase pairs of all channels for cue-left and cue-right conditions, and this was done for both multi and single stimuli cases. The resulting plots can be seen for all subjects in Figure 7. As expected, in the single stimulus trials there is a clear 180 degree phase offset between cue-right and cue-left responses. It seems there is no common pattern in the amplitude-phase shifts for the multi-stimuli responses with respect to the single-stimuli case. This suggests that the multi-stimuli SSVEPs are not only the result of a combination of the original single-stimuli waves with amplitude modulations, but also that phase changes are required to lead to the resulting multi-stimuli waves.

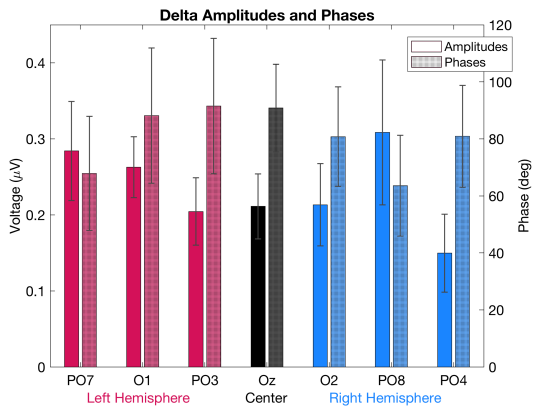

Fig. 6: Averages, across subjects, of the absolute values of the differences in SSVEP amplitudes and phases between cue-left and cue-right time-domain-averaged trials for each scalp site. Error bars represent standard errors.

B. Real-Time CVSA Classification

A real-time CVSA classification was simulated offline using the features obtained from the epochs given by a moving window as explained in Section II-G. Resulting test accuracies for unseen data are shown in Figure 8. The line for each subject represents the averaged accuracy computed from the 10-fold cross validation. The mean accuracy across subjects reaches 88.4 $\pm$ 8%, with a maximum accuracy of 98% for Subject 2. Subjects 7 and 8 show significantly lower performance than the rest. SNR, number of trials rejected and number of feature vectors used for the classifier were analyzed for these two subjects. Neither of these variables accounted for the accuracy differences with respect to the other subjects.

IV. Discussion and Conclusion

This paper studies the effects of covert spatial attention on the SSVEPs using single-frequency phase-coded stimuli. The present findings suggest that the topography of the phase-coded SSVEP responses across the scalp is sensitive to spatially focused attention. Therefore, we have demonstrated the feasibility of utilizing phase-coded stimuli to discriminate where in the visual field the subject is covertly attending to.

Amplitude-phase pairs of all channels shift towards the same direction in the polar plane, and all cortical regions experience statistically comparable changes ($p > 0.05$) in both SSVEP amplitudes and phases when switching the side of attention. The direction of the amplitude-phase shift is variable and subject-dependent. Trials with single-stimulus were run so the evoked cortical responses could be compared with the multi-stimuli SSVEPs. Results show that, across subjects, there is no common pattern in the amplitude-phase shifts for the multi-stimuli responses with respect to the single-stimuli case. This suggests that the multi-stimuli SSVEPs are not only the result of a combination of the original single-stimuli waves with amplitude modulations, but also that phase changes are required to lead to the resulting multi-stimuli waves. Similar effects were observed

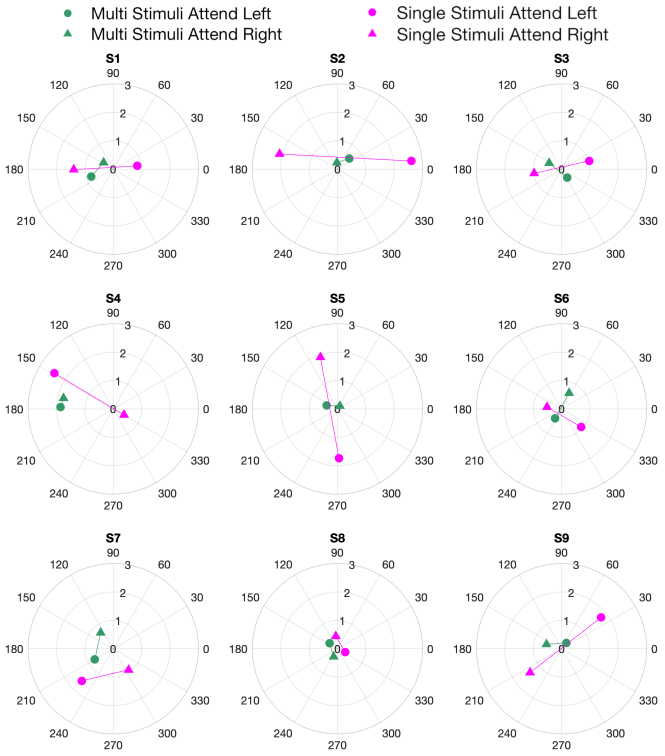

Fig. 7: Centroids of amplitude-phase pairs of all channels for cue-left or cue-right. Single-stimuli trials in pink, multi-stimuli in green.

in [13], where there could be seen a shift in SSVEP phases at many scalp sites between the attended and the unattended conditions in a frequency-coded stimuli experiment.

A pseudo real-time CVSA classification was explored offline by exploiting the topography of the SSVEP responses. The amplitude and phase of the SSVEPs – fundamental and first harmonic – at each scalp site were used as features to train a logistic regression classifier on each subject. The system achieved an average classification accuracy of 88.4 $\pm$ 8% on unseen data. To the best of our knowledge, this is the first time a system has been shown to discriminate covert visuo-spatial attention in (pseudo) real-time using SSVEP from phase-coded stimulation.

The discovery that the SSVEPs to 15Hz phase-coded stimuli can be modulated by covert attention opens the door to utilizing this modulation in applications that track CVSA. This finding can largely increase the number of targets by adopting more efficient coding techniques such as the joint frequency-phase modulation.

Future work will consist on exploring if similar effects take place in higher frequency bands, as well as examining the maximum number of phases that can be encoded in a unique frequency. As far as the real-time approach, more sophisticated algorithms can be used going forward, such as task-related component analysis (TRCA) [34], or xDAWN algorithm [35], which can help to improve the SNR and hence the system performance.

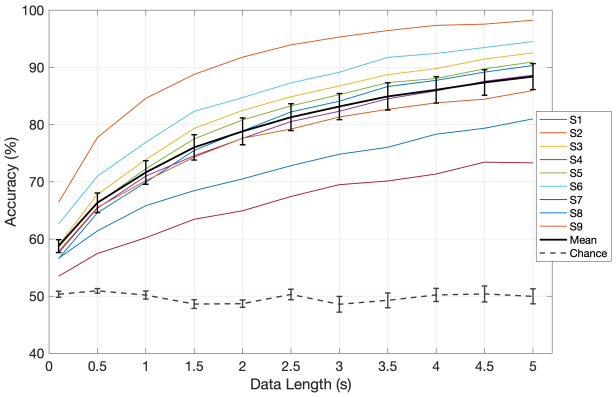

Fig. 8: Classification accuracy for unseen data as a function of data length used to extract amplitude and phase features. Chance curve represents the classifier accuracy with randomly shuffled labels. The error bars represent standard errors.

REFERENCES

[1] M. I. Posner, "Orienting of attention," Quarterly journal of experimental psychology, vol. 32, no. 1, pp. 3–25, 1980.

[2] M. Carrasco, C. Penpeci-Talgar, and M. Eckstein, "Spatial covert attention increases contrast sensitivity across the CSF: support for signal enhancement," Vision research, vol. 40, no. 10-12, pp. 1203–1215, 2000.

[3] W. Prinzmetal, H. Amiri, K. Allen, and T. Edwards, "Phenomenology of attention: I. color, location, orientation, and spatial frequency.," Journal of Experimental Psychology: Human Perception and Performance, vol. 24, no. 1, p. 261, 1998.

[4] Y. Yeshurun and M. Carrasco, "The locus of attentional effects in texture segmentation," nature neuroscience, vol. 3, no. 6, pp. 622–627, 2000.

[5] K. Nakayama and M. Mackeben, "Sustained and transient components of focal visual attention," Vision research, vol. 29, no. 11, pp. 1631–1647, 1989.

[6] R. Hasan, R. Srinivasan, and E. D. Grossman, "Feature-based attentional tuning during biological motion detection measured with SSVEP," Journal of vision, vol. 17, no. 9, pp. 22–22, 2017.

[7] V. C. Chu and M. D'Zmura, "Tracking feature-based attention," Journal of neural engineering, vol. 16, no. 1, p. 016022, 2019.

[8] C. Jeunet, L. Tonin, L. Albert, R. Chavarriaga, B. Bideau, F. Argelaguet, J. d. R. Millán, A. Lécuyer, and R. Kulpa, "Uncovering EEG correlates of covert attention in soccer goalkeepers: towards innovative sport training procedures," Scientific Reports, vol. 10, no. 1, pp. 1–16, 2020.

[9] S. Morgan, J. Hansen, and S. Hillyard, "Selective attention to stimulus location modulates the steady-state visual evoked potential," Proceedings of the National Academy of Sciences, vol. 93, no. 10, pp. 4770–4774, 1996.

[10] Y. J. Kim, M. Grabowecky, K. A. Paller, K. Muthu, and S. Suzuki, "Attention induces synchronization-based response gain in steady-state visual evoked potentials," Nature neuroscience, vol. 10, no. 1, pp. 117–125, 2007.

[11] C. S. Herrmann, "Human EEG responses to 1–100 Hz flicker: resonance phenomena in visual cortex and their potential correlation to cognitive phenomena," Experimental brain research, vol. 137, no. 3-4, pp. 346–353, 2001.

[12] S. A. Hillyard, H. Hinrichs, C. Tempelmann, S. T. Morgan, J. C. Hansen, H. Scheich, and H.-J. Heinze, "Combining steady-state visual evoked potentials and fMRI to localize brain activity during selective attention," Human brain mapping, vol. 5, no. 4, pp. 287–292, 1997.

[13] M. M. Müller, T. W. Picton, P. Valdes-Sosa, J. Riera, W. A. Teder-Sälejärvi, and S. A. Hillyard, "Effects of spatial selective attention on the steady-state visual evoked potential in the 20–28 Hz range," Cognitive brain research, vol. 6, no. 4, pp. 249–261, 1998.

[14] S. P. Kelly, E. C. Lalor, C. Finucane, G. McDarby, and R. B. Reilly, "Visual spatial attention control in an independent brain-computer interface," IEEE transactions on biomedical engineering, vol. 52, no. 9, pp. 1588–1596, 2005.

[15] S. P. Kelly, E. C. Lalor, R. B. Reilly, and J. J. Foxe, "Visual spatial attention tracking using high-density ssvep data for independent brain-computer communication," IEEE Transactions on Neural Systems and Rehabilitation Engineering, vol. 13, no. 2, pp. 172–178, 2005.

[16] S. K. Andersen, M. M. Müller, and S. A. Hillyard, "Color-selective attention need not be mediated by spatial attention," Journal of Vision, vol. 9, no. 6, pp. 2–2, 2009.

[17] W. Zhang and S. J. Luck, "Feature-based attention modulates feedforward visual processing," Nature neuroscience, vol. 12, no. 1, pp. 24–25, 2009.

[18] J.-M. Hopf, K. Boelmans, M. A. Schoenfeld, S. J. Luck, and H.-J. Heinze, "Attention to features precedes attention to locations in visual search: evidence from electromagnetic brain responses in humans," Journal of Neuroscience, vol. 24, no. 8, pp. 1822–1832, 2004.

[19] T. Liu, J. Larsson, and M. Carrasco, "Feature-based attention modulates orientation-selective responses in human visual cortex," Neuron, vol. 55, no. 2, pp. 313–323, 2007.

[20] M. Müller, S. Andersen, N. Trujillo, P. Valdes-Sosa, P. Malinowski, and S. Hillyard, "Feature-selective attention enhances color signals in early visual areas of the human brain," Proceedings of the National Academy of Sciences, vol. 103, no. 38, pp. 14250–14254, 2006.

[21] D. Zhang, A. Maye, X. Gao, B. Hong, A. K. Engel, and S. Gao, "An independent brain–computer interface using covert non-spatial visual selective attention," Journal of neural engineering, vol. 7, no. 1, p. 016010, 2010.

[22] T. Sakurada, T. Kawase, T. Komatsu, and K. Kansaku, "Use of high-frequency visual stimuli above the critical flicker frequency in a ssvep-based bmi," Clinical neurophysiology, vol. 126, no. 10, pp. 1972–1978, 2015.

[23] A. Armengol-Urpi and S. E. Sarma, "Sublime: a hands-free virtual reality menu navigation system using a high-frequency ssvep-based brain-computer interface," in Proceedings of the 24th ACM Symposium on Virtual Reality Software and Technology, pp. 1–8, 2018.

[24] L. Jiang, Y. Wang, W. Pei, and H. Chen, "A four-class phase-coded SSVEP BCI at 60Hz using refresh rate," in 2019 41st Annual International Conference of the IEEE Engineering in Medicine and Biology Society (EMBC), pp. 6331–6334, IEEE, 2019.

[25] F. W. Gembler, A. Rezeika, M. Benda, and I. Volosyak, "Five shades of grey: exploring quintary m-sequences for more user-friendly c-vep-based bcis," Computational Intelligence and Neuroscience, vol. 2020, 2020.

[26] S. A. Hillyard and L. Anllo-Vento, "Event-related brain potentials in the study of visual selective attention," Proceedings of the National Academy of Sciences, vol. 95, no. 3, pp. 781–787, 1998.

[27] E. E. Sutter, "The brain response interface: communication through visually-induced electrical brain responses," Journal of Microcomputer Applications, vol. 15, no. 1, pp. 31–45, 1992.

[28] Y. Wang, X. Gao, B. Hong, C. Jia, and S. Gao, "Brain-computer interfaces based on visual evoked potentials," IEEE Engineering in medicine and biology magazine, vol. 27, no. 5, pp. 64–71, 2008.

[29] P.-L. Lee, J.-J. Sie, Y.-J. Liu, C.-H. Wu, M.-H. Lee, C.-H. Shu, P.-H. Li, C.-W. Sun, and K.-K. Shyu, "An ssvep-actuated brain computer interface using phase-tagged flickering sequences: a cursor system," Annals of biomedical engineering, vol. 38, no. 7, pp. 2383–2397, 2010.

[30] X. Mao, W. Li, H. Hu, J. Jin, and G. Chen, "Improve the classification efficiency of high-frequency phase-tagged SSVEP by a recursive bayesian-based approach," IEEE Transactions on Neural Systems and Rehabilitation Engineering, vol. 28, no. 3, pp. 561–572, 2020.

[31] Neuroelectrics, Neuroelectrics Enobio, accessed September 2020. https://www.neuroelectrics.com/solutions/enobio.

[32] D. H. Brainard, "The psychophysics toolbox," Spatial vision, vol. 10, no. 4, pp. 433–436, 1997.

[33] Z. Yan, X. Gao, and S. Gao, "Right-and-left visual field stimulation: A frequency and space mixed coding method for ssvep based brain-computer interface," Science China Information Sciences, vol. 54, no. 12, pp. 2492–2498, 2011.

[34] M. Nakanishi, Y. Wang, X. Chen, Y.-T. Wang, X. Gao, and T.-P. Jung, "Enhancing detection of ssveps for a high-speed brain speller using task-related component analysis," IEEE Transactions on Biomedical Engineering, vol. 65, no. 1, pp. 104–112, 2017.

[35] B. Rivet, A. Souloumiac, V. Attina, and G. Gibert, "xdawn algorithm to enhance evoked potentials: application to brain–computer interface," IEEE Transactions on Biomedical Engineering, vol. 56, no. 8, pp. 2035–2043, 2009.